Journal of Medicinal Chemistry Article

J. Med. Chem. **2010,** *53,* 5667–5675 **5667**
DOI: 10.1021/jm1004072

m-Azipropofol (AziP*m*) a Photoactive Analogue of the Intravenous General Anesthetic Propofol

Michael A. Hall,[‡] Jin Xi,[†] Chong Lor,[§] Shuiping Dai,[§] Robert Pearce,[§] William P. Dailey,[‡] and Roderic G. Eckenhoff*[,†]

[†]*Department of Anesthesiology and Critical Care, and* [‡]*Department of Chemistry, University of Pennsylvania School of Medicine, Philadelphia, Pennsylvania, and* [§]*Department of Anesthesiology, University of Wisconsin, Madison, Wisconsin*

Received March 31, 2010

Propofol is the most commonly used sedative-hypnotic drug for noxious procedures, yet the molecular targets underlying either its beneficial or toxic effects remain uncertain. In order to determine targets and thereby mechanisms of propofol, we have synthesized a photoactivateable analogue by substituting an alkyldiazirinyl moiety for one of the isopropyl arms but in the meta position. *m*-Azipropofol retains the physical, biochemical, $GABA_A$ receptor modulatory, and in vivo activity of propofol and photoadducts to amino acid residues in known propofol binding sites in natural proteins. Using either mass spectrometry or radiolabeling, this reagent may be used to reveal sites and targets that underlie the mechanism of both the desirable and undesirable actions of this important clinical compound.

Introduction

Propofol (2,6-diisopropylphenol) is the most widely used intravenous general anesthetic agent for induction and maintenance of anesthesia as well as sedation for procedures and in the critically ill patient.[1] Although more potent than the inhaled anesthetics, propofol's micromolar EC_{50} and lipophilicity still predict only brief interactions with its in vivo targets. This is considered clinically useful because it allows for short duration of action once administration is stopped. Unfortunately, these transient interactions make the molecular targets of general anesthetics difficult to study. The use of photoaffinity labeling has emerged as a promising technique for investigating these otherwise fleeting interactions.[2]

A molecular target that is thought to contribute to propofol's ability to induce anesthesia is the $GABA_A$[a] receptor, a ligand-gated chloride channel responsible for the majority of inhibitory signaling in the brain. Propofol both activates $GABA_A$ receptors and potentiates the activity of receptors activated by GABA; these activities correlate with its in vivo anesthetic potency.[3−5] However, the precise molecular interactions between propofol and the $GABA_A$ receptor remain unclear. Photoactive compounds that mimic propofol's mechanism of action would allow a greater understanding of the mechanisms.

In addition to studies directed at known propofol targets, a propofol photoaffinity label could be used for identifying other molecular targets of this drug, both desirable and undesirable. These studies would facilitate medicinal chemistry aimed at favoring targets underlying effects such as induction of anesthesia, anticonvulsant effects, and reduction of cerebral blood flow and metabolic rate[1,6] and disfavoring those targets underlying propofol's toxicities. Most notable of these toxicities would be respiratory depression and cardiac dysfunction, including bradycardia and hypotension,[7] and also EEG activation and even seizures.[8,9] Here we describe the synthesis and characterization of a propofol analogue with an alkyldiazirinyl group in place of one of the isopropyl arms.

Results

An obvious position for introduction of a photoactivatable group into propofol would be as part of one of the existing isopropyl groups in propofol itself. However, we recognized that these positions, by virtue of being ortho to the phenolic hydroxyl group, would likely lead to *intra*molecular reaction of the active position with the hydroxyl group rather than the desired *inter*molecular reaction with proteins. Therefore, we designed our propofol photoaffinity probe to contain the photoactivatable group in a meta position relative to the hydroxyl group. This design would preclude any intramolecular reaction of the reactive site with the phenolic hydroxyl group.

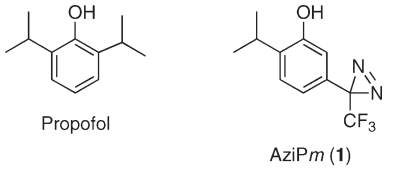

Synthesis of *m*-Azipropofol (AziP*m*, 1). Synthesis of **1** is shown is Scheme 1. Cumene (**2**) is treated with bromine in the presence of a catalytic amount of iodine to give known bromo compound **3**, which is treated with magnesium followed by *N*-trifluoroacetylpyrrolidine to give the previously reported trifluoroacetylbenzene **4**. Nitration conditions provide nitro compound **5**, which is reduced under catalytic hydrogenation conditions to give aniline **6**. Conversion of **6**

*To whom correspondence should be addressed. Address: Department of Anesthesiology and Critical Care, 311a John Morgan Building, 3620 Hamilton Walk, Philadelphia, PA 19104. Phone: 215-662-3705. Fax: 215-349-5078. E-mail: Roderic.eckenhoff@uphs.upenn.edu.

[a] Abbreviations: AziP*m*, *m*-azipropofol; 1-AMA, 1-aminoanthracene; HSAF, horse spleen apoferritin; $GABA_A$, γ-aminobutyric acid receptor type A, EEG, electroencephalograph; ITC, isothermal titration calorimetry; MEM, minimal essential media.

Published on Web 07/02/2010

Scheme 1

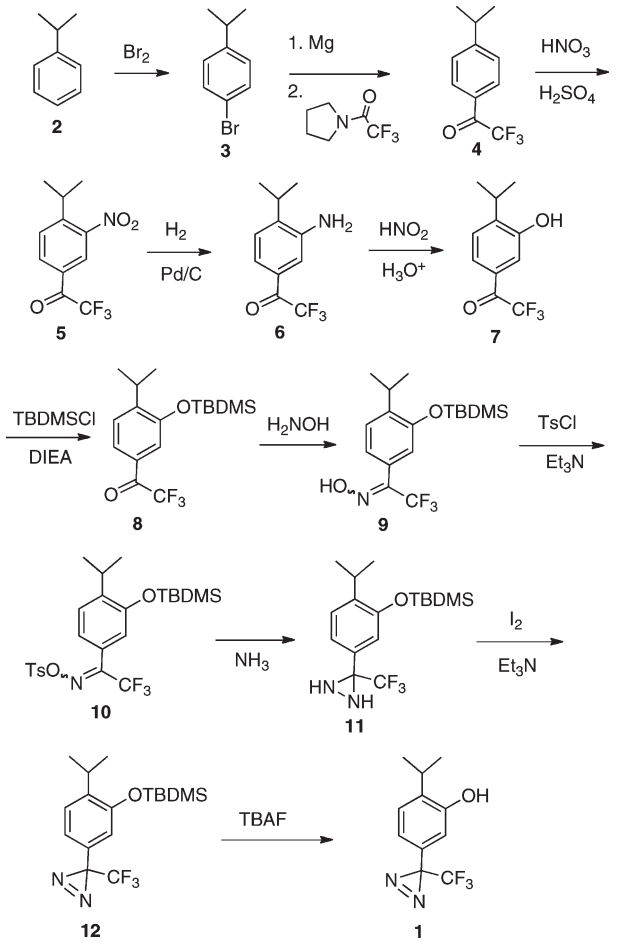

to phenol **7** is accomplished using nitrous acid and boiling aqueous acid. Subsequent protection of the free phenol group using the *tert*-butyldimethylsilyl protecting group provides **8**. Introduction of the diazirine group into ketone **8** closely followed a method previously described for a similar ketone.[10] Thus, conversion to oxime **9** and oxime tosylate **10** followed standard procedures. Treating **10** with ammonia produces diaziridine **11**, which is oxidized with iodine and triethylamine to produce diazirine **12**. Deprotection of the *tert*-butyldimethylsilyl group occurs under standard fluoride conditions to give **1** in an overall yield of 18% starting with cumene.

Physicochemical Properties. The physicochemical properties for both **1** and propofol are summarized in Table 1. The octanol/water partition coefficients of **1** (log *P*) and propofol were calculated to be 3.93 and 3.79, respectively. Density of **1** was determined to be 1.12 g/mL. The calculated molecular dipole for **1** was 2.12 D, while the dipole for propofol, calculated the same way, was 1.70 D. The UV absorption spectrum demonstrates a prominent diazirine peak at 368 nm with an extinction coefficient (Σ_{368}) of 670/M. Because of this absorption profile, all photolysis was done with a 350 nm UV lamp. The rate of disappearance of the diazirine during irradiation in a cuvette, as measured by changes in the UV spectrum, has a $t_{1/2}$ of 34 min (95% CI = 31−37 min). The maximum concentration of **1** achievable in distilled water was found to be 185 μM.

Binding Assays. Equilibrium binding of **1** to horse spleen apoferritin (HSAF) was determined by two methods, ITC and fluorescence competition, and the results are provided in Table 2 and in Figures 1 and 2. There existed good agreement across methods and across the two compounds. Propofol had a 2- to 4-fold higher affinity for HSAF than did **1**. In the photo-occlusion experiments, a 40% reduction in 1-AMA fluorescence was noted when compared to control HSAF samples that were identically treated but without the addition of **1** (Figure 3). Combined, these results support the proposition that **1** binds the anesthetic pocket of HSAF[11] rather than inner filter effects explaining the competition results.

Table 1. Physicochemical Properties

	MW	density, g/mL	log P[a]	dipole,[a] D	HSAF K_D, μM
1	244	1.12	3.93	2.12	19
propofol	178	0.96	3.79	1.70	10

[a] Calculated; see Experimental Procedures. log P = octanol/water partition coefficient.

Table 2. Binding Parameters

	1		propofol	
	ITC	fluorescence competition	ITC	fluorescence competition
affinity[a]	21 (20−22)	23 (17, 32)	4.8 (3.9−6.5)	12 (9, 15)
Hill slope	1[b]	−1.2 (−0.9, −1.6)	1[b]	−1.0 (−0.8, −1.2)

[a] Mean (95% CI), in μM. [b] Data fitted to single class binding site, so Hill slope fixed at 1.

In Vivo Anesthetic Potency. Both **1** and propofol showed anesthetic activity in *X. laevis* tadpoles by reversibly extinguishing both spontaneous and elicited (startle reflex) movement. The results of these assays are summarized in Table 3 and presented in Figure 4. The Hill slopes and EC_{50} values for the two compounds had overlapping 95% confidence intervals for all measurements, indicating similar potencies in tadpoles. The only difference noted during the trials was that propofol had more rapid kinetics; it reached its maximum effect in about half of the time that it took **1** to reach steady state. Also, it was found that neither compound had a concentration that immobilized 100% of the tadpoles (loss of startle response) reversibly. This suggested a very narrow therapeutic ratio for both compounds, which was confirmed to be less than 2. The EC_{50} reported here for propofol in *Xenopus* tadpoles agrees with previously reported values, despite subtle differences in methodology.[4]

Electrophysiological Studies. We compared effects of propofol and **1** on $\alpha1\beta2\gamma2$L $GABA_A$ receptors expressed in HEK293 cells. At 0.3 and 3 μM, both compounds reversibly enhanced responses of receptors activated by 3 μM GABA (in fold changes, propofol 5.1 ± 3 and 9.3 ± 7.1; **1** 1.8 ± 0.1 and 1.7 ± 0.4; $p < 0.05$ for all). In addition, propofol but not **1** directly activated receptors; i.e., current flow was produced even in the absence of GABA. At the highest concentration tested (30 μM), propofol strongly activated receptors. By contrast, 30 μM **1** did not directly activate receptors, and receptor activation in the combined presence of 30 μM **1** and GABA was reduced or eliminated. However, upon removal of **1** and GABA, there was a modest "rebound" or tail current. This pattern of responses has been suggested to arise from direct channel block by anesthetics.[12]

Photolabeling. In order to confirm the ability of **1** ability to act as a photolabel, HSAF was incubated in buffer with and without saturated (185 μM) **1** and exposed to 350 nm illumination for 20 min. Concentration and trypsinization were followed by nano-LC/MS to identify peptides and residues

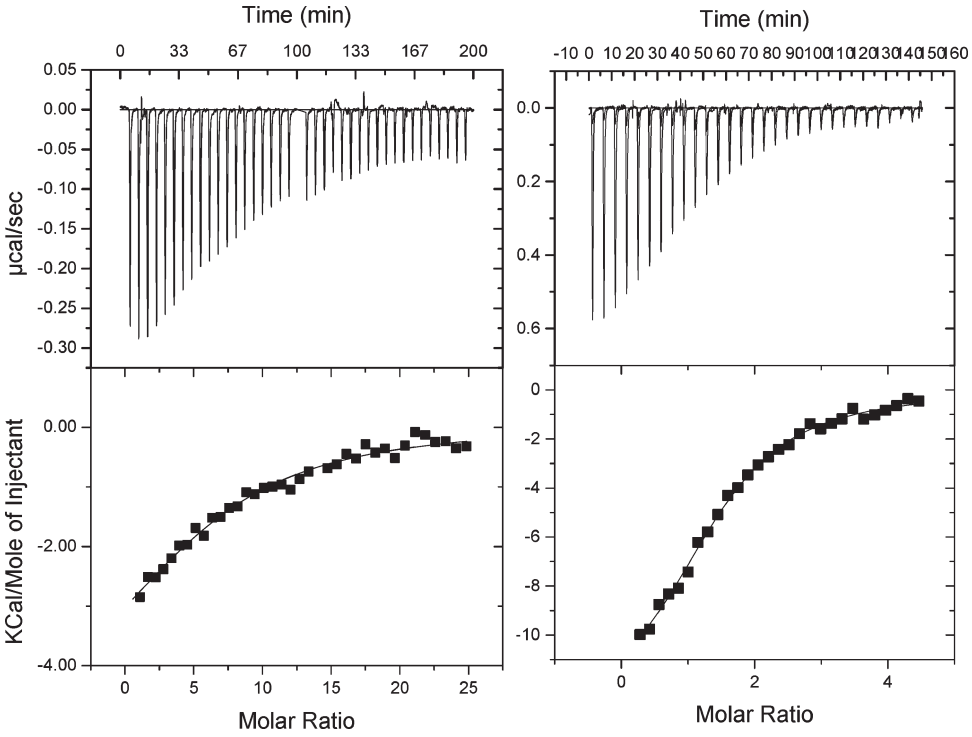

Figure 1. Isothermal titration calorimetry of the HSAF interaction with either **1** (left) or propofol (right), using sequential titrations. More sigmoid shaped curve with propofol indicates higher affinity, consistent with the values given in Table 2.

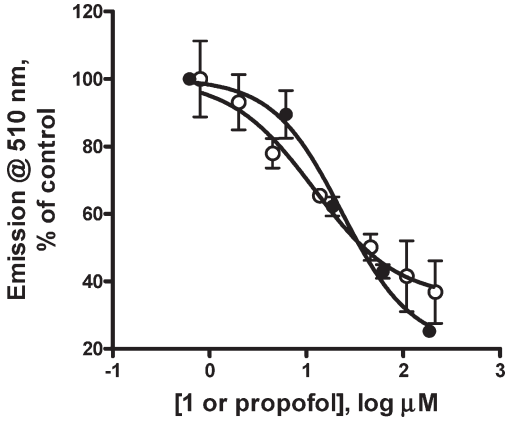

Figure 2. Fluorescence competition with 1-aminoanthracene. Titration of the HSAF/1-AMA combination with either **1** (filled symbols) or propofol (open symbols) produced inhibition of fluorescence consistent with competition for binding. Lines represent nonlinear least-squares fits to variable slope Hill functions. Values are given in Table 2.

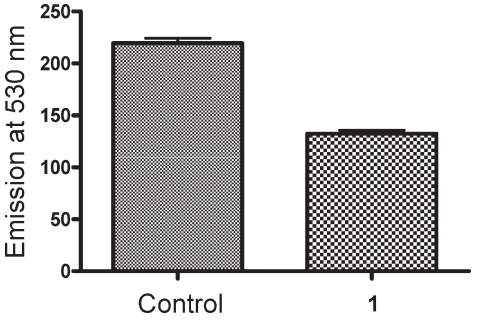

Figure 3. Photo-occlusion experiment. In order to confirm that fluorescence competition was not due to inner filter or other nonspecific interactions between 1-AMA, **1**, and HSAF, the protein was photoadducted by **1**/UV, washed, and then evaluated for 1-AMA binding via fluorescence enhancement. The photoadducted sample had significantly reduced 1-AMA binding compared to the UV control, consistent with adduction in the 1-AMA anesthetic binding site.

that had been modified by 216 Da (**1** without the dinitrogen). We detected peptides covering 42.9% of the apoferritin sequence. The HSAF L chain demonstrated clear evidence of two adducted peptides. MS/MS sequencing indicated that the adducts were located at leucine-81 and leucine-24, both of which are known to be lining residues in the previously identified propofol binding cavity (see Supporting Information and Figure 6).[11]

Discussion and Conclusions

In order to create a photolabel analogue of propofol, we initially decided to incorporate an alkyldiazirine functional group after the success of creating the smaller azi-isoflurane.[2] On the basis of previous investigations into the anesthetic potency of various alkyl-substituted phenols,[13] we chose to substitute the alkyldiazirine for one of the isopropyl groups while leaving the other isopropyl in the 2-position on the ring.

This decision produced the possibility of synthesizing a series of azi-propofols, varying in which position on the ring carried the diazirine group. While the ortho-azi-propofol would demonstrate the greatest steric similarity to propofol, the concern that the compound would internally rearrange after diazirine decomposition instead of photolabeling made this a less attractive initial objective. The rearrangement of similar aromatic compounds into the corresponding ortho-quinone methanides has been described.[14] With this potential for decomposition via an intramolecular pathway, we were concerned about the effectiveness as a photolabel. Therefore,

Table 3. Tadpole Studies Results

	1, endpoint		propofol, endpoint	
	spontaneous movement	startle reflex	spontaneous movement	startle reflex
EC_{50}[a] (μM)	1.1 (0.9−1.4)	3.1 (2.7−3.5)	1.1 (0.9−1.3)	2.8 (2.6−3.0)
Hill slope	2.8 (1.6−4.0)	2.9 (1.7−4.1)	2.7 (1.6−3.9)	3.0 (2.4−3.7)

[a] Values in parentheses is the 95% confidence interval.

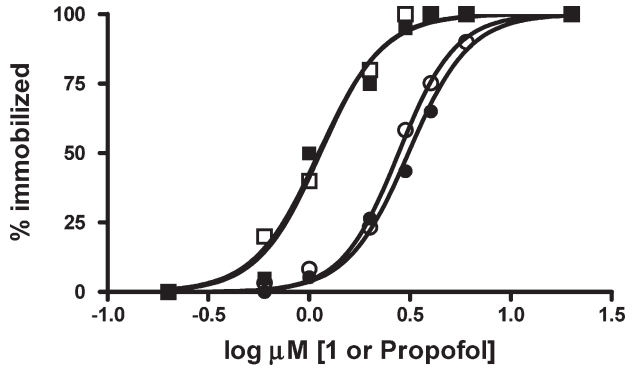

Figure 4. In vivo dose/response relationships. Tadpoles were evaluated with two end points: spontaneous (left set of curves, squares) and elicited (right set of curves, circles) movement. Filled symbols represent **1**, and open symbols are propofol data. No significant differences between the two drugs could be detected for either end point.

after ruling out the ortho compound and considering that previously reported[13] structural analogues of the meta- and para-compounds retained anesthetic potency, we chose to synthesize the meta-compound **1** first.

Subsequent attempts to synthesize the para-azi-propofol (AziP*p*) using the synthetic strategy outlined in Scheme 1 failed in the final, deprotecting step. We hypothesized that this occurred because the base-catalyzed deprotection creates a phenoxide intermediate. The phenoxide is conjugated with the diazirine in such a way that the diazirine decomposes immediately; evolved N_2 gas was observed during the addition of the tetrabutylammonium fluoride. Attempts to synthesize AziP*p* using a methoxymethyl protecting group, which is removed under acid conditions, were only marginally more successful. Any synthesized AziP*p* was seen to rapidly decompose when isolation was attempted. Diazirines conjugated with phenols are known to be very unstable under basic conditions,[15] and with this conjugation potentially lowering the pK_a of the molecule below that of phenol, we expect there to be significant decomposition and loss of photolabeling functionality when AziP*p* is added to the pH 7.4 phosphate buffered saline in which the HSAF experiments are performed. Hence, **1** was synthesized as described herein.

From a comparison of **1** to propofol, the diazirine exchange for the isopropyl adds 66 Da to the molecular weight and increases the dipole considerably, from 1.70 to 2.12 D, but still makes the compound marginally more hydrophobic, with log *P* changing from 3.79 to 3.93. Even with these changes, in vitro and in vivo binding studies indicate that **1** is a highly analogous and similarly potent anesthetic when compared to propofol. The **1**/HSAF interaction was found to be of slightly lower affinity compared to propofol/HSAF, but their EC_{50} values for anesthetizing tadpoles were not different. Both compounds also enhanced agonist-stimulated activity of the $GABA_A$ receptor complex at concentrations near those that impaired movement (<3 μM), with **1** being less potent. This is consistent with previous work on propofol analogues where loss of bulk from the 6-position or transfer of bulk from the ortho to meta or para resulted in loss of potency.[4] It is of interest that this lower potency at $GABA_A$ receptors is also reflected in the HSAF affinity but not in the in vivo potency. Previous work has shown that the relationship between $GABA_A$ enhancement in heterologous expression systems and tadpole immobilization only explains about half the variation,[4] so it is possible that additional molecular targets of propofol and **1** are contributing to immobilization in the tadpole.

Alternatively, the ability of high concentration **1** to block the $GABA_A$ complex (Figure 5) may indicate the recruitment of additional, low affinity sites within this ion channel because of the electrophysiological signature for channel blockade at high (lethal) concentrations. Such a functionally antagonistic site would be expected to reduce the coagonist actions of the propofol site, as was observed. Finally, it is unlikely that receptor blockade underlies lethality, since both propofol and **1** were similarly lethal in tadpoles. Nevertheless, the ability of **1** to block receptors may provide a new tool for understanding the origin of channel block at high concentrations, a feature of other anesthetics.[12,16,17]

The photolabeling experiment demonstrates that both **1** and propofol are recognized as similar by a protein and that **1** has the ability to act as a photoaffinity label. The competition and occlusion studies had already suggested that **1** binds in the propofol-binding cavity of HSAF. The photolabeling experiment identified that the **1** binding site was within labeling distance of two residues, leucine-81 and leucine-24, which are adjacent to each other and contribute to the lining of the previously identified propofol binding site of HSAF.[11] This confirms that **1** binds within the same cavity that propofol (and inhaled anesthetics) binds, making this compound a promising photolabel for studies of propofol binding in other potential drug targets. We cannot rule out that adduction took place in 57% of the protein sequence for which peptides were not identified, but we consider this unlikely because only a single propofol site has been found with crystallography[11] and the ITC and 1-AMA competition data for **1** are analogous to the data for propofol and give no indication of additional binding sites. The fact that affinity of the **1**/HSAF interaction predicted the lowered efficacy for $GABA_A$ enhancement is further evidence that the HSAF site bears strong architectural and physicochemical similarity to the site underlying allosteric enhancement in $GABA_A$ receptors.

Current application of **1** requires detection using mass spectrometry. While this is useful for detecting adducted peptides within proteins, it is less useful for detecting novel targets in complex mixtures or anatomic regions of the brain or heart that might have a high density of targets. Thus, a future direction for this work involves incorporating a radioactive moiety into **1**. For example, [^{3}H]**1** could be synthesized by iodination of the aromatic ring followed by catalytic

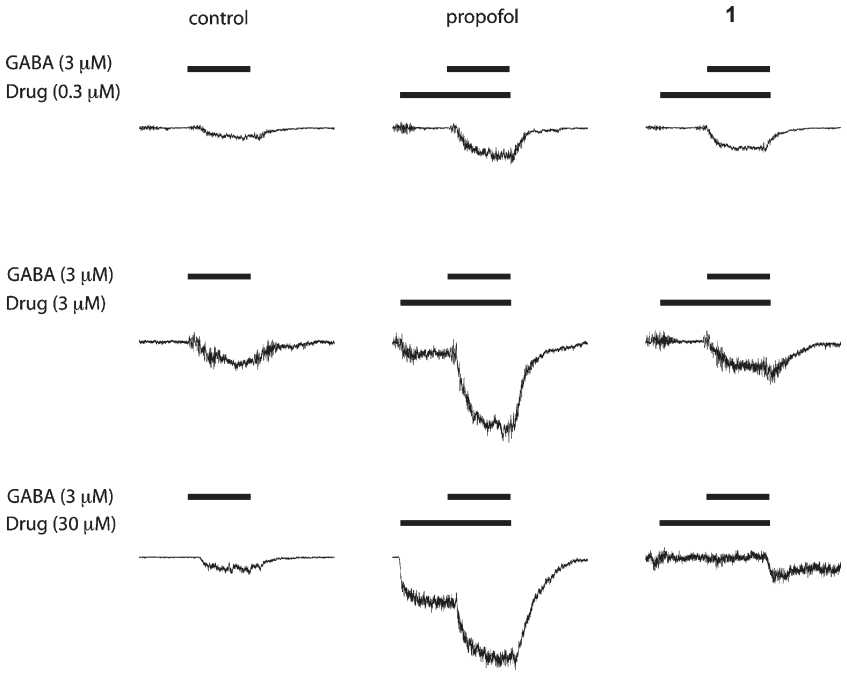

Figure 5. Electrophysiology in $GABA_A$ receptors. Excised patches containing $\alpha1\beta2\gamma2L$ receptors were exposed to 3 μM GABA alone (left column) or together with propofol (middle column) or **1** (right column) for 500 ms. At 0.3 and 3 μM, both compounds enhanced responses to GABA. At a high concentration (30 μM), propofol directly activated channels, whereas **1** blocked channels.

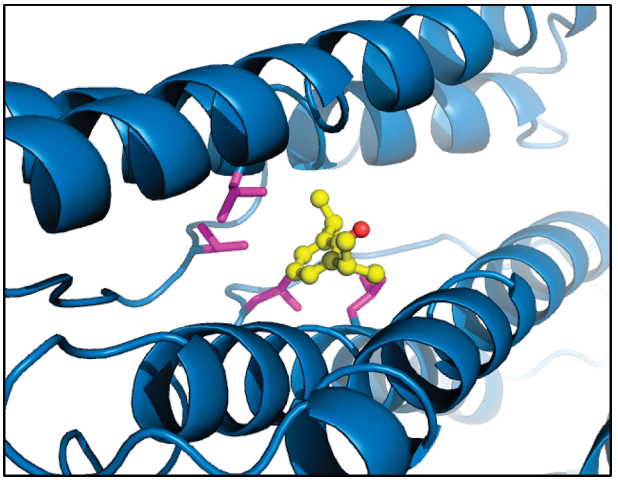

Figure 6. Adducted HSAF residues. Shown is the HSAF anesthetic binding site with propofol bound (yellow), from PDB code 3F33. Residues photolabeled by **1** (L24 and L81 from each of two monomers) (pink) are immediately adjacent to propofol. Mass spectra are provided in the Supporting Information.

hydrogenation to replace the iodine with tritium, using $[^3H]_2$ gas as the source.

Experimental Procedures

Physicochemical Properties. The density of **1** was calculated from the slope of the volume/mass relationship of this low-volatility compound. The UV spectrum and extinction coefficient of the diazirine absorption were first determined from a methanolic solution of **1** of known concentration, and then maximal water solubility was calculated from the extinction coefficient. The rate of photolysis was determined from a 160 μM solution in distilled water in a 1 cm path length quartz cuvette in contact with a 350 nm UV light for 30 min, taking UV spectra to monitor the disappearance of the diazirinyl peaks every 3 min. Octanol/water partition coefficients were calculated using XLOGP3.[18]

Electronic structure calculations at the ab initio RHF/6-31+G(d,p) geometry optimized level demonstrate two conformations with 160 cal/mol difference as the lowest energy conformations.[19] These two conformations differ in rotation of 180° about the bond between the diazirine carbon and the aromatic ring such that the plane of the ring bisects the diazirine double bond in both conformations. This indicates relatively free rotation of the diazirine group relative to the aromatic ring. The dipole moment calculated for each of these conformations was found to be 1.99 and 2.25 D. With total energies so close, we assumed that these conformations would contribute equally to the total dipole at room temperature, giving **1** a dipole of 2.12 D. The same calculations for propofol demonstrated fairly free rotation about bonds connecting each isopropyl group to the aromatic ring, creating several minima with different individual dipole moments. Consideration of a Maxwell−Boltzmann distribution for the total energy of each conformation at room temperature allowed the calculation of an average dipole of 1.70 D, as the individual dipoles ranged between 1.67 and 1.80 D.

Binding Studies. Fluorescence Competition. The affinity of **1** for HSAF was determined by adding increasing amounts of **1** to a solution of HSAF and a constant amount of 1-aminoanthracene (1-AMA).[20] All solutions were prepared in pH 7.4 phosphate buffered saline. In 500 μL quartz cuvettes, 7 μM HSAF and 7 μM 1-AMA were combined with increasing concentrations of **1** (0−110 μM). The fluorescence of 1-AMA in each of these solutions was determined with 380 nm excitation while monitoring emission between 400 and 800 nm. The fluorescence curves were corrected by subtracting the baseline fluorescence curves of 1-AMA and HSAF. The fluorescence intensity vs concentration data were fitted to variable slope Hill models to obtain the IC_{50} and Hill slope. The K_D was then calculated using the Cheng−Prusoff equation to correct the IC_{50} for the presence of the 1-AMA competitor.[20]

Photo-Occlusion. To ensure that the measured effect of **1** on the fluorescence of 1-AMA in HSAF was indeed caused by competition for the anesthetic-binding pocket of HSAF rather than an inner-filter effect of **1**, a photo-occlusion experiment

was performed. In 1 mL quartz cuvettes, 5 μM HSAF with or without 140 μM **1** in pH 7.4 phosphate buffered saline was irradiated with 350 nm light (Rayonet RPR-3500 lamp) at 2 mm distance for 20 min. Both samples were then passed through a PD-10 buffer exchange column to remove any remaining soluble **1** or unadducted photolysis products. HSAF solutions were returned to the quartz cuvettes, and baseline fluorescence curves were obtained for the **1** sample, the irradiated control, and a control that had not been irradiated. There was no significant change in fluorescence between the two controls, indicating a lack of appreciable UV damage to the HSAF. To each of the irradiated HSAF samples was added 1-AMA (3 μM final concentration), and fluorescence was recorded. Occlusion of the anesthetic (1-AMA) binding site by adducted **1** is reflected by a significant loss of fluorescence in the **1**/UV sample.

Isothermal Titration Calorimetry. The thermodynamics of **1**'s interaction with HSAF was assessed by isothermal titration calorimetry using a Microcal, Inc. VP ITC (Northampton, MA; http://www.microcalorimetry.com) and compared to that of propofol. The ITC consists of a matched pair of sample and reference vessels (1.43 mL) enclosed in an adiabatic enclosure and a rotating stirrer-syringe for titrating aliquots of the ligand solution into the sample vessel. The sample cell contained 5 μM HSAF, and the reference cell contained water. Saturated photolabel (185 μM) was loaded in the syringe (volume of 0.28 mL) for injecting into the sample. Because of the low solubility of these ligands, sequential titrations were employed to achieve sufficient molar ratios for reliable model fitting, and these titrations were linked using ConCat32 software (Microcal, Inc., Northampton, MA). In addition to these sequential titrations, control titrations were performed, including ligand into buffer, buffer into protein, and buffer into buffer, which were then used to correct the experimental titration, ligand into protein. Origin 5.0 (Microcal Software, Inc., Northampton, MA) was used to fit thermodynamic parameters to the heat profiles using a single binding site class.

Tadpole Studies. In vivo activity studies were performed in *Xenopus* tadpoles. Groups of 10 tadpoles were placed in 30 mL of pond water containing various concentrations of **1** or propofol. Tadpoles were incubated in the pond water with compound for 30 min to allow for full equilibration, regardless of the progress toward immobilization. At the end of the 30 min, the anesthetic effect was assessed using two end points. The first was loss of spontaneous motion, defined as the percentage of tadpoles at each dose that did not swim, right themselves, or twitch in a 30 s observation. The second end point was loss of elicited movement to a single, sharp tap on the lid of their dish. Tadpoles that did not twitch or swim in response to this stimulus were scored as anesthetized. The water in the dish was then replaced with fresh pond water, and recovery was observed over the next 24 h.

Photolabeling. Small aliquots of pH 7.0 phosphate buffer containing ~5 μM HSAF with and without saturated (185 μM) **1** were placed in 300 μL, 1 mm path length quartz cuvettes and exposed to 350 nm light (Rayonet RPR-3500 lamp) at <2 mm distance for 20 min. Control samples received only UV irradiation. Samples were washed and concentrated with 50 kDa centrifuge filters and then trypsinized and injected into a nano-LC/MS (10 cm C18 capillary column) to separate and identify the digested peptides. Eksigent NanoLC proteomics experiments were run at 200 nL/min for 60 min with gradient elution. Nanospray was used to spray the separated peptides into LTQ (Thermo Electron). Xcalibur was used to acquire the raw data, and modified (photolabeled) peptides were identified using Sequest. Mass spectrometry equipment and software were available in the Proteomics Core Facility at the University of Pennsylvania.

Electrophysiology. HEK293 Cell Culture and $GABA_A$ Receptor Expression. HEK293 cells (CRL 1573, American Type Culture Collection) were maintained in standard culture conditions (37 °C, 5% CO_2) in culture medium consisting of minimum essential medium (MEM) with L-glutamine and Earle's salts (Gibco), supplemented with MEM amino acids solution (0.1 mM), sodium pyruvate (1 mM), 1% penicillin/streptomycin, and 10% fetal bovine serum (Harlan). For transfection, cDNAs for rat $GABA_A$ receptor α1, β2, and γ2L subunits were subcloned into the multiple cloning site of the mammalian expression vector pUNIV.[21] For receptor expression, cells were plated onto 60 mm culture dishes (Corning). After incubation for 24−48 h, cells were co-transfected with rat $\alpha1\beta2\gamma2$L (1:1:10) and 100 ng of pCEP4-EGFP (Clontech) using Lipofectamine 2000 (Invitrogen), then replated onto a 12 mm circle cover glass in 35 mm Petri dishes (Falcon) 12−16 h after transfection. Transfected cells were identified using a mercury arc lamp and a GFP filter cube (Chroma Technology).

Electrophysiological Recordings. Recordings were performed at room temperature on the stage of an inverted microscope. Solutions were applied to excised outside-out patches or whole cells using a custom-designed 12-barrel application system constructed of Teflon (28 gauge) and polyimide tubing (Cole-Parmer). The tubes were sealed together and glued onto a microscope slide using UV curing glue (Norland optical adhesive) and secured in place using epoxy. The barrels were individually connected to solution reservoirs (10 mL glass syringes) using Teflon tubing and valves. The application system was mounted on a motorized scanning stage (Corvus). An open-tip solution exchange time constant of 20−30 ms was typically achieved. The recording chamber was perfused continuously with HEPES-buffered saline containing the following (mM): NaCl 145, KCl 5, $MgCl_2$ 1, $CaCl_2$ 1.8 HEPES 10; pH 7.4. Recording electrodes were fabricated from KG-33 glass (Garner Glass Company) using a multistage puller (model P-87, Sutter Instruments). The tips were fire-polished; open tip electrode resistance was typically 4−7 MΩ when filled with standard recording solution. Recording pipettes were filled with the following (mM): KCl 130, EGTA 5, HEPES 10, $MgCl_2$ 1, MgATP 5; pH 7.2. All recordings were obtained at a holding potential of −40 mV using an Axopatch 200A amplifier (Molecular Devices). GABA solutions were prepared fresh daily from powder and were diluted to the desired concentration (3 μM) in HEPES-buffered saline solution. Propofol and **1** solutions were prepared by diluting stock solutions containing 0.53 mM propofol and 0.18 mM azipropofol in HEPES-buffered saline solution.

Data Analysis. Ionic currents were analyzed using Clampfit 10 (Molecular Devices) and Origin 7.5 (OriginLab, Northampton, MA). Peak currents were measured relative to baseline and normalized to the peak current elicited by a pulse of 3 μM GABA. Data are presented as mean ± SD.

General Synthetic Procedures. All reagents and solvents were used as received from commercial sources unless otherwise noted. ^{1}H, ^{13}C, and ^{19}F NMR spectra were recorded on a Bruker DMX 360 MHz nuclear magnetic resonance spectrometer. ^{1}H, ^{13}C, and ^{19}F NMR spectra are in the Supporting Information. Determination of the final purity of **1** used capillary GC (30 m × 0.25 mm DB-5 column, 135 °C injector, 200 °C detector, column temperature of 100 °C for 25 min, then 10 °C/min to 200 °C) using flame ionization detection. Under these conditions **1** has a retention time of ~25 min and was shown to be >98% pure by integration.

2-Isopropyl-5-[3-(trifluoromethyl)-3*H*-diazirin-3-yl]phenol (1). To a round-bottom flask with a magnetic stir bar was added 466.8 mg (1.30 mmol) of **12** and 5 mL of dry THF. The solution was cooled in an ice bath, and 1.45 mL (1.45 mmol) of TBAF (1.0 M in THF) was added dropwise via syringe over 5 min. The reaction mixture was allowed to warm and stir for 20 min at room temperature. The mixture was poured into 20 mL of saturated NH_4Cl and extracted with methylene chloride. The organic layers were combined, washed with water, and dried with Na_2SO_4. Solvent was removed under reduced pressure, and the residue was purified on silica gel (20:1 hexanes/ethyl acetate).

Evaporation of the solvent yielded 279.1 mg (88%) of **1** as a pale-yellow oil which was one spot by TLC. ^{1}H NMR: δ 7.25 (d, J = 10.6 Hz, 1H), 6.72 (d, J = 8.1 Hz, 1H), 6.60 (bs, 1H), 4.97 (s, 1H), 3.21 (septet, J = 6.9 Hz, 1H), 1.25 ppm (d, J = 6.9 Hz, 6H). ^{19}F NMR: δ −65.27 ppm. ^{13}C NMR: δ 152.9, 136.5, 127.7, 127.1, 122.1 (q, J = 274 Hz), 119.1, 113.3, 28.2 (q, J = 40 Hz), 27.0, 22.2 ppm. UV spectrum: λ_{max} = 282, 368 nm. HRMS (ESI neg): m/z calcd for $C_{11}H_{10}F_3N_2O$ $(M - H)^-$, 243.0745; found, 243.0746.

1-Bromo-4-isopropylbenzene (3). A 500 mL round-bottom flask with a magnetic stir bar was filled with 10.0 g (39.4 mmol) of iodine crystals and 80.0 g (667 mmol) of isopropylbenzene. The solution was cooled in an ice bath, and 110.0 g (688 mmol) of bromine was added over 15 min with good stirring. A solution of 60.0 g (1.07 mol) of potassium hydroxide in 200 mL of H_2O was added to the mixture. The reaction mixture was steam-distilled for 12 h, with periodic addition of fresh water. The organic layer of the distillate was dried over $MgSO_4$ and then distilled at atmospheric pressure to give 108.9 g (82%) of a clear, colorless liquid, bp 217 °C (lit. bp 216 °C).[22] ^{1}H NMR: δ 7.44 (2H, d, J = 8.4 Hz), 7.13 (2H, d, J = 8.3), 2.85 (1H, septet), 1.27 ppm (6H, d, J = 6.9 Hz).

2,2,2-Trifluoro-1-(4-isopropylphenyl)ethanone (4). In a three-neck round-bottom flask with a magnetic stir bar, 23.28 g (117 mmol) of **3** was dissolved in 115 mL of dry THF. To this solution was added 2.87 g (118 mmol) of magnesium metal. The reaction vessel was fitted with a condenser topped with a nitrogen line and an addition funnel containing 15.66 g (101 mmol) of 2,2,2-trifluoro-1-pyrrolidin-1-ylethanone in 24 mL of dry THF. The pot was heated slowly to reflux, and heating was continued for 20 min after the magnesium began to react to ensure complete consumption of **3**. The flask was cooled in an ice/salt bath for 25 min, during which time a fine, white precipitate formed. The amide solution was added dropwise over 30 min at 0 °C to the well stirred solution. After the addition was complete, the ice/salt bath was removed, and the mixture was stirred at room temperature for 1 h. The reaction was quenched with 30 mL of saturated aqueous NH_4Cl solution and then vacuum-filtered to leave a clear, golden liquid. After the mixture was dried over $MgSO_4$, solvent was removed under reduced pressure. Distillation under aspirator pressure yielded 16.20 g (74%) of **4**, bp_{13} 95 °C (lit. bp_{15} 95 °C).[23] ^{1}H NMR: δ 8.03 (2H, d, J = 7.6 Hz), 7.41 (2H, d, J = 7.7 Hz), 3.05 (1H, septet), 1.31 ppm (6H, d, J = 6.9 Hz). ^{19}F NMR: δ −71.73 ppm.

2,2,2-Trifluoro-1-(4-isopropyl-3-nitrophenyl)ethanone (5). In a beaker with a magnetic stir bar, an amount of 44.50 g of concentrated H_2SO_4 was added dropwise to 16.18 g (74.9 mmol) of **4** at −10 °C over 25 min, during which time a red precipitate formed. While the temperature was maintained below −5 °C, a mixture of 10.84 g of concentrated HNO_3 and 20.66 g of concentrated H_2SO_4 was added dropwise over 25 min. The ice/salt bath was replaced with an ice/water bath, and the mixture was allowed to stir for 1 h. The reaction mixture was poured onto 200 g of ice and was extracted with ether (3 × 100 mL). The ether fractions were combined and washed with saturated aqueous $NaHCO_3$ until no more CO_2 was generated. The ether layer was dried over anhydrous $MgSO_4$, and the solvent was removed under reduced pressure. The resulting oil was distilled under aspirator pressure to give 17.17 g (88%) of **5**, bp_{15} 140 °C. ^{1}H NMR: δ 8.39 (1H, s), 8.23 (1H, d), 7.72 (1H, d, J = 8.4 Hz), 3.47 (1H, septet), 1.36 ppm (6H, d, J = 6.8 Hz). ^{19}F NMR: δ −72.39 ppm. ^{13}C NMR: δ 178.6 (q, J = 37 Hz), 150.3, 150.1, 133.0, 128.9, 128.4, 125.4, 116.4 (q, J = 289 Hz), 29.2, 23.1 ppm. HRMS (CI+): m/z calcd for $C_{11}H_{11}NO_3F_3$(M + H) 262.0691; found 262.0691.

1-(3-Amino-4-isopropylphenyl)-2,2,2-trifluoroethanone (6). A round-bottom flask with a magnetic stir bar was filled with 26.50 g (101.5 mmol) of **5** dissolved in 160 mL of glacial acetic acid. To this solution was added 68 mg of 30% Pt on asbestos along with 511 mg of 10% activated Pd on carbon. The mixture was stirred under a 1 atm hydrogen atmosphere at room temperature for 2 days. The mixture was filtered through Celite, and the residue was rinsed with 95% ethanol. The combined ethanol and acetic acid were removed under reduced pressure to give **6** in quantitative yield. ^{1}H NMR: δ 7.37 (1H, s), 7.49 (1H, d, J = 8.1 Hz), 7.30 (1H, d), 3.60 (2H, broad s), 2.95 (1H, septet), 1.31 ppm (6H, d, J = 6.8 Hz). ^{19}F NMR: δ −71.49 ppm. ^{13}C NMR: δ 180.4 (q, J = 34 Hz), 144.2, 141.0, 128.3, 126.1, 120.9, 116.8 (q, J = 295 Hz), 116.1, 28.1, 21.7 ppm. HRMS (CI+): m/z calcd for $C_{11}H_{13}NOF_3(M + H^+)$ 232.0949; found 232.0939.

2,2,2-Trifluoro-1-(3-hydroxy-4-isopropylphenyl)ethanone (7). A large beaker with a magnetic stir bar and thermocouple was filled with 20.44 g (88.4 mmol) of **6** and a solution of 31.0 mL of concentrated H_2SO_4 and 24.0 mL of water. This mixture was cooled to 0 °C, and a solution of 9.16 g (133 mmol) of $NaNO_2$ in 23.0 mL of H_2O was added dropwise over the course of 90 min, taking care to keep the temperature of the mixture below 4 °C. Once the addition was complete, this mixture was poured in several small additions over 30 min through a condenser into a round-bottom flask containing a refluxing solution of 68 mL of concentrated H_2SO_4 and 90 mL of H_2O. Additional water was used to rinse out the beaker. Once the addition was complete, the mixture was allowed to reflux for an additional 15 min before being poured into 1 L of cold water, at which point a dark oil separated. The mixture was extracted with ether, and the ether was washed with water, dried over $MgSO_4$, and removed at reduced pressure to leave 16.14 g (79%) of crude **7**. This black oil was taken to the next step without further purification. An analytical sample was prepared by multiple sublimations under reduced pressure, mp 58−60 °C. ^{1}H NMR: δ 7.64 (1H, d), 7.48 (1H, s), 7.38 (1H, d), 3.35 (1H, sep), 1.31 ppm (6H, d). ^{19}F NMR: δ −71.59 ppm. ^{13}C NMR: δ 180.2 (q, J = 34 Hz), 153.4, 144.2, 128.4, 127.2, 123.4, 116.7 (q, J = 295 Hz), 115.9, 27.6, 22.0 ppm. HRMS (CI+): m/z calcd for $C_{11}H_{11}F_3O_2Na$ (M + Na), 255.0609; found, 255.0605.

1-[3-(*tert*-Butyldimethylsilanyloxy)-4-isopropylphenyl]-2,2,2-trifluoroethanone (8). To a round-bottom flask with a magnetic stir bar was added 10.78 g (46.4 mmol) of **7**, 250 mL of dry THF, 12.2 g (94.5 mmol) of diisopropylethylamine, and 16.92 g (112.4 mmol) of *tert*-butyldimethylchlorosilane. This mixture was stirred for 24 h under nitrogen atmosphere at room temperature. The mixture was poured into 500 mL of H_2O and extracted with methylene chloride. The combined organic phase was washed with water, and volatiles were removed under vacuum. Crude **8** was purified through a short column of silica, eluting with pure hexanes to give 7.62 g (47%) of **8** as an oil. ^{1}H NMR: δ 7.67 (1H, bd), 7.50 (1H, bs), 7.38 (1H, d, J = 8 Hz), 3.40 (1H, septet), 1.25 (6H, d, J = 7 Hz), 1.06 ppm (9H, s). ^{19}F NMR: δ −71.2 (s). ^{13}C NMR: δ 179.8 (q, J = 34 Hz), 153.3, 148.4, 128.3, 126.9, 123.4, 118.9, 116.9 (q, J = 290 Hz), 27.2, 25.7, 22.2, 18.2 ppm. HRMS-(CI+): m/z calcd for $C_{17}H_{26}F_3O_2Si$ (M^+), 347.1654; found, 347.1653.

1-[3-(*tert*-Butyldimethylsilanyloxy)-4-isopropylphenyl]-2,2,2-trifluoroethanone Oxime (9). To a round-bottom flask with a magnetic stir bar was added 6.87 g (19.8 mmol) of **8**, 1.75 g (25.2 mmol) of hydroxylamine hydrochloride, and 50 mL of pyridine. The mixture was heated in an oil bath to 60 °C and stirred for 4 h under nitrogen atmosphere. Volatiles were then removed under vacuum. The remaining crude product was partitioned between methylene chloride and water, and the organic phase was subsequently washed with water. Solvent was removed under vacuum to leave 6.82 g (95%) of **9** as an approximately 1:1 mixture of oxime diastereomers as determined by NMR. The crude product was taken to the next step without further purification. An analytical sample was prepared by flash chromatography on silica gel (10:1 hexanes/ethyl acetate, $R_f \approx 0.3$). ^{1}H NMR: δ 9.4 (1H, bs), 7.32 (0.6H, d, J = 8 Hz), 7.27 (0.4H, d, J = 8 Hz), 7.18 (0.6H, bd), 7.09 (0.4H, bd), 7.06 (0.6H, bs), 6.93 (0.4H, bs), 3.37 (1H, m), 1.24 (6H, m), 1.06 (9H, s), 0.28 ppm (6H, s). ^{19}F NMR: δ −62.3 (1F, s), −66.3 ppm (1.2F, s). ^{13}C NMR: δ 152.8, 152.7, 147.8, 147.4, 147.3, 147.0, 142.2, 142.0, 127.8, 126.5, 126.4,

123.5, 122.3, 121.6, 120.0, 119.2, 118.5, 118.0, 116.9, 26.8, 26.7, 25.8, 25.7, 22.6, 22.5, 18.2, −4.2, −4.3 ppm. HRMS(CI+): *m*/*z* calcd for $C_{17}H_{27}F_3NO_2Si$ (M^+), 362.1763; found 362.1780.

1-[3-(*tert*-Butyldimethylsilanyloxy)-4-isopropylphenyl]-2,2,2-trifluoroethanone Oxime Tosylate (10). A round-bottom flask with a magnetic stir bar was filled with 5.75 g (15.9 mmol) of **9** and 110 mL of methylene chloride. To this stirred solution was added 93 mg (0.76 mmol) of 4-(*N*,*N*-dimethylamino)pyridine, 3.18 g (16.7 mmol) of *p*-toluenesulfonyl chloride, and 2.20 g (21.8 mmol) of triethylamine. The mixture was stirred for 24 h under nitrogen atmosphere at room temperature. The reaction mixture was then partitioned between water and methylene chloride, and the organic phase was subsequently washed with additional water. Volatiles were removed under vacuum to leave 7.50 g (91%) of crude **10** as a 2:3 mixture of diastereomers as determined by NMR. This crude product was taken to the next step without further purification. An analytical sample was prepared by flash chromatography on silica gel (20:1 hexanes/ethyl acetate) and was followed by TLC in 10:1 hexanes/ethyl acetate, R_f = 0.4, to give **10** as a thick gum. ^{1}H NMR: δ 7.95 (2H, m), 7.4 (2H, m), 7.32 (0.6H, d), 7.28 (0.4H, d), 7.07 (1H, m), 6.97 (0.6H, m), 6.91 (0.4H, m), 3.38 (1H, m), 2.47 (3H, m), 1.24 (3H, m), 1.07 (9H,m), 0.31 (3.4H, s), 0.26 ppm (2.6H, s) ^{19}F NMR: δ −61.2 (2F), −66.1 ppm (3F). ^{13}C NMR: δ 153.5, 153.2, 152.9, 152.8, 146.1, 145.9, 143.8, 143.6, 131.7, 131.4, 129.9, 129.8, 129.1, 126.8, 126.7, 125.6, 122.2, 121.8, 119.1, 118.5, 115.9, 31.6, 26.8, 26.8, 25.7, 22.6, 22.4, 21.65, 18.3, 18.2, 14.0, −4.3 ppm. HRMS(CI+): *m*/*z* calcd for $C_{24}H_{33}F_3NO_4SSi$ ($M + H^+$), 516.1852; found 516.1835.

3-[3-(*tert*-Butyldimethylsilanyloxy)-4-isopropylphenyl]-3-trifluoromethyldiaziridine (11). A solution of 7.50 g (14.5 mmol) of **10** dissolved in 15.0 g of diethyl ether was added to excess liquid ammonia at −78 °C and stirred vigorously as it was allowed to come to room temperature over the course of 5 h. More ether was added to the reaction mixture, and the combined organic phase was washed with water. The ether solution was dried over Na_2SO_4, and solvent was removed under reduced pressure to leave 5.13 g (98%) of crude **11**. The crude product could be taken to the next step without further purification. An analytical sample was prepared by flash column chromatography (hexanes/ethyl acetate = 20:1) followed by TLC in the same solvent system with an R_f of 0.25 to give **11** as a thick oil. ^{1}H NMR: δ 7.26 (1H, d, J = 6.6 Hz), 7.20 (1H, d, J = 6.6 Hz), 7.065 (1H, s), 3.34 (1H, m, J = 5.7 Hz), 2.75 (1H, broad s), 2.20 (1H, broad d, J = 5.7 Hz), 1.24 (6H, d), 1.06 (9H, s), 0.28 ppm (6H, s). ^{19}F NMR: δ −75.43 ppm. ^{13}C NMR: δ 152.78, 141.25, 129.60, 128.17, 126.56, 123.5 (q, J = 278 Hz), 120.45, 117.78, 57.66 (q, J = 36 Hz), 26.61, 25.74, 25.73, 22.64, 22.61, 18.25, −4.22, −4.27 ppm. HRMS (CI+): *m*/*z* calcd for $C_{17}H_{28}F_3N_2OSi$ (M^+), 361.1923; found, 361.1926.

3-[3-(*tert*-Butyldimethylsilanyloxy)-4-isopropylphenyl]-3-trifluoromethyl-3*H*-diazirine (12). A round-bottom flask with a magnetic stir bar was filled with 5.35 g (14.8 mmol) of crude **11**, 40 mL of methylene chloride, and 5.8 g (22.9 mmol) of iodine. The mixture was cooled in an ice bath, and 4.57 g (45.2 mmol) of triethylamine was added dropwise. The ice bath was removed, and the mixture was allowed to stir at room temperature for 45 min. It was poured into 650 mL of 1 M NaOH and was stirred vigorously for 15 min. The mixture was extracted with methylene chloride. The organic layer was washed with water and evaporated under reduced pressure. The resultant crude product was flushed through a short column of silica with pure hexanes to give 3.10 g (58%) of **12** as a yellow oil. ^{1}H NMR: δ 7.22 (1H, d, J = 8.1 Hz), 6.70 (1H, s), 6.63 (1H, d, J = 8.1 Hz), 3.30 (1H, sep, J = 6.9 Hz), 1.19 (6H, d, J = 6.9 Hz), 1.04 (9H, s), 0.27 ppm (6H, s). ^{19}F NMR: δ −65.67 ppm. ^{13}C NMR: δ 153.1, 141.1, 127.2, 126.8, 122.2 (q, J = 275 Hz), 118.9, 116.4, 28.2 (q, J = 40 Hz), 26.6, 25.7, 22.5 18.2, −4.3 ppm. HRMS(CI+): *m*/*z* calcd for $C_{17}H_{26}F_3N_2OSi$ (M^+), 359.1767; found, 359.1762. The column was then flushed with an equal volume of 10:1 hexanes/ethyl acetate to recover 1.78 g of unreacted **11**.

Acknowledgment. The authors declare no conflicts of interest. This work was supported by NIH Grants GM055876 (R.G.E.), MH84836 (R.G.E.), and NS056411 (R.P.) and the Wisconsin Institutes for Discovery Seed Grant (R.P.).

Supporting Information Available: NMR spectra of compounds and mass spectra of protein. This material is available free of charge via the Internet at http://pubs.acs.org.

References

(1) Kotani, Y.; Shimazawa, M.; Yoshimura, S.; Iwama, T.; Hara, H. The experimental and clinical pharmacology of propofol, an anesthetic agent with neuroprotective properties. *CNS Neurosci. Ther*. **2008**, *14*, 95–106.
(2) Eckenhoff, R. G.; Xi, J.; Shimaoka, M.; Bhattacharji, A.; Covarrubias, M.; Dailey, W. P. Azi-isoflurane, a photolabel analog of the commonly used inhaled general anesthetic isoflurane. *ACS Chem. Neurosci*. **2010**, *1*, 139–145.
(3) Eghbali, M.; Gage, P. W.; Birnir, B. Effects of propofol on GABAA channel conductance in rat-cultured hippocampal neurons. *Eur. J. Pharmacol*. **2003**, *468*, 75–82.
(4) Krasowski, M. D.; Jenkins, A.; Flood, P.; Kung, A. Y.; Hopfinger, A. J.; Harrison, N. L. General anesthetic potencies of a series of propofol analogs correlate with potency for potentiation of γ-aminobutyric acid (GABA) current at the $GABA_A$ receptor but not with lipid solubility. *J. Pharmacol. Exp. Ther*. **2001**, *297*, 338–351.
(5) Trapani, G.; Latrofa, A.; Franco, M.; Altomare, C.; Sanna, E.; Usala, M.; Biggio, G.; Liso, G. Propofol analogues. Synthesis, relationships between structure and affinity at $GABA_A$ receptor in rat brain, and differential electrophysiological profile at recombinant human $GABA_A$ receptors. *J. Med. Chem*. **1998**, *41*, 1846–1854.
(6) Rajda, C.; Dereczyk, D.; Kunkel, P. Propofol infusion syndrome. *J. Trauma Nurs*. **2008**, *15*, 118–122.
(7) Orsini, J.; Nadkarni, A.; Chen, J.; Cohen, N. Propofol infusion syndrome: case report and literature review. *Am. J. Health-Syst. Pharm*. **2009**, *66*, 908–915.
(8) Smith, M.; Smith, S. J.; Scott, C. A.; Harkness, W. F. Activation of the electrocorticogram by propofol during surgery for epilepsy. *Br. J. Anaesth*. **1996**, *76*, 499–502.
(9) Baraka, A.; Aouad, M. Is propofol anticonvulsant or proconvulsant? *Can. J. Anaesth*. **1997**, *44*, 1027–1028.
(10) Furuta, T.; Ueda, M.; Hirooka, Y.; Tanaka, K.; Kan, T. Synthesis of diazirine possessing an acetophenone derivative as a valuable intermediate for a flavonoid photoaffinity probe. *Heterocycles* **2008**, *76*, 811–817.
(11) Vedula, L. S.; Brannigan, G.; Economou, N. J.; Xi, J.; Hall, M. A.; Liu, R.; Rossi, M. J.; Dailey, W. P.; Grasty, K. C.; Klein, M. L.; Eckenhoff, R. G.; Loll, P. J. A unitary anesthetic-binding site at high resolution. *J. Biol. Chem*. **2009**, *284*, 24176–24184.
(12) Haseneder, R.; Rarnmes, G.; Zieglgansberger, W.; Kochs, E.; Hapfelmeier, G. $GABA_A$ receptor activation and open-channel block by volatile anaesthetics: a new principle of receptor modulation? *Eur. J. Pharmacol*. **2002**, *451*, 43–50.
(13) James, R.; Glen, J. B. Synthesis, biological evaluation, and preliminary structure−activity considerations of a series of alkylphenols as intravenous anesthetic agents. *J. Med. Chem*. **1980**, *23*, 1350–1357.
(14) Katada, T.; Eguchi, S.; Esaki, T.; Sasaki, T. Thermal cycloaddition reactions of thiocarbonyl compounds. Part 3. A novel [4 + 2] cycloaddition reaction of thiocarbonyl compounds with *o*-quinone methanides. *J. Chem. Soc., Perkin Trans. 1* **1984**, 2649–2653.
(15) Hatanaka, Y.; Hashimoto, M.; Nakayama, H.; Kanaoka, Y. Syntheses of nitro-substituted aryl diazirines. An entry to chromogenic carbene precursors for photoaffinity labeling. *Chem. Pharm. Bull*. **1994**, *42*, 826–831.
(16) Akk, G.; Steinbach, J. H. Activation and block of recombinant GABA(A) receptors by pentobarbitone: a single-channel study. *Br. J. Pharmacol*. **2000**, *130*, 249–258.
(17) Li, P.; Covey, D. F.; Steinbach, J. H.; Akk, G. Dual potentiating and inhibitory actions of a benz[*e*]indene neurosteroid analog on recombinant alpha1beta2gamma2 GABAA receptors. *Mol. Pharmacol*. **2006**, *69*, 2015–2026.
(18) Cheng, T. J.; Zhao, Y.; Li, X.; Lin, F.; Xu, Y.; Zhang, X. L.; Li, Y.; Wang, R. X. Computation of octanol−water partition coefficients by guiding an additive model with knowledge. *J. Chem. Inf. Model*. **2007**, *47*, 2140–2148.
(19) Frisch, M. J.; Trucks, G. W.; Schlegel, H. B.; Scuseria, G. E.; Robb, M. A.; Cheeseman, J. R.; Scalmani, G.; Barone, V.; Mennucci, B.; Petersson, G. A.; Nakatsuji, H.; Caricato, M.; Li, X.; Hratchian,

H. P.; Izmaylov, A. F.; Bloino, J.; Zheng, G.; Sonnenberg, J. L.; Hada, M.; Ehara, M.; Toyota, K.; Fukuda, R.; Hasegawa, J.; Ishida, M.; Nakajima, T.; Honda, Y.; Kitao, O.; Nakai, H.; Vreven, T.; Montgomery, J. A., Jr.; Peralta, J. E.; Ogliaro, F.; Bearpark, M.; Heyd, J. J.; Brothers, E.; Kudin, K. N.; Staroverov, V. N.; Kobayashi, R.; Normand, J.; Raghavachari, K.; Rendell, A.; Burant, J. C.; Iyengar, S. S.; Tomasi, J.; Cossi, M.; Rega, N.; Millam, N. J.; Klene, M.; Knox, J. E.; Cross, J. B.; Bakken, V.; Adamo, C.; Jaramillo, J.; Gomperts, R.; Stratmann, R. E.; Yazyev, O.; Austin, A. J.; Cammi, R.; Pomelli, C.; Ochterski, J. W.; Martin, R. L.; Morokuma, K.; Zakrzewski, V. G.; Voth, G. A.; Salvador, P.; Dannenberg, J. J.; Dapprich, S.; Daniels, A. D.; Farkas, O.; Foresman, J. B.; Ortiz, J. V.; Cioslowski, J.; Fox, D. J. *Gaussian 09*, revision A.02; Gaussian, Inc.: Wallingford, CT, 2009.

(20) Butts, C. A.; Xi, J.; Brannigan, G.; Saad, A. A.; Venkatachalan, S. P.; Pearce, R. A.; Klein, M. L.; Eckenhoff, R. G.; Dmochowski, I. J. Identification of a fluorescent general anesthetic, 1-amino-anthracene. *Proc. Natl. Acad. Sci. U.S.A.* **2009**, *106*, 6501–6506.

(21) Venkatachalan, S. P.; et al. Optimized expression vector for ion channel studies in Xenopus oocytes and mammalian cells using alfalfa mosaic virus. *Pfluegers Arch.* **2007**, *454*, 155–163.

(22) Simchen, G.; Schmidt, A. A simple method for the preparation of aryl trifluoromethyl ketones. *Synthesis* **1996**, *9*, 1093–1094.

(23) Harrison, C. R.; Hodge, P.; Hunt, B. J.; Khoshdel, E.; Richardson, G. Preparation of alkyl chlorides, acid chlorides, and amides using polymer-supported phosphines and carbon tetrachloride: mechanism of these reactions. *J. Org. Chem.* **1983**, *48*, 3721–3728.